Journal of Civil Engineering and Urban Planning (2026)
Clausius Scientific Press, Canada

DOI: 10.23977/jceup.2026.080207
ISSN 2616-3969 Vol. 8 Num. 2

Comparative seismic analysis of MRD and BRB for structural control under sequential earthquakes

Haifan Zhu

Key Laboratory of Urban Security and Disaster Engineering of Ministry of Education, Beijing University of Technology, Beijing, 100124, China

Keywords: Sequential earthquakes; Seismic performance; Magnetorheological damper; Buckling-restrained brace; Dynamic analysis

Abstract: Structural safety is a critical concern under sequential earthquakes. Buckling-restrained braces (BRBs), as an effective damping solution, have been widely adopted in the construction industry. However, under long-duration and high-intensity seismic events, BRBs may undergo ultimate axial failure or fatigue failure. This study investigates the efficacy of magnetorheological dampers (MRDs) for seismic response mitigation. A comparative analysis is conducted between 3-story and 9-story reinforced concrete (RC) frames equipped with BRBs and those equipped with MRDs, under sequential seismic events. The results demonstrate that MRDs can effectively mitigate seismic responses and significantly reduce structural acceleration during frequent earthquakes, thereby enhancing residential comfort. In two consecutive rare earthquakes, MRDs exhibit superior performance and stability in controlling inter-story drift and top-floor residual deformations, alongside excellent energy dissipation capacity.

1. Introduction

Earthquakes are sudden and catastrophic natural disasters that pose a significant threat to human life and property [1-2]. Extensive seismic sequence data reveal that numerous aftershocks occur shortly after the main shock, some of which exhibit considerable magnitudes. Moreover, several studies have demonstrated that successive seismic events can lead to a significant increase in structural damage compared to the damage caused by a single earthquake event [3-5]. Hatzivassiliou et al. [6] investigated the inelastic response of irregular RC structures, comprising two three-story and two five-story buildings, and revealed that multiple earthquakes can significantly increase the demand for ductility in individual components. Amiri et al. [7] analyzed six moment RC frames with varying story heights under two different seismic records, and indicated that seismic sequences can nearly double the accumulated structural damage and amplify the seismic response of structures. Wen et al. [8] evaluated the loss of resilience in RC structures due to aftershocks, considering the recovery time and pre-event functionality of the system, and demonstrated that aftershocks could exacerbate resilience loss when compared to the mainshock alone.

Traditional earthquake-resistant methods typically rely on high-strength materials and large components; however, these approaches are costly and may result in structural damage [9]. With advancements in technology and seismic theory, the installation of energy dissipation and isolation

components to absorb and dissipate the energy generated by seismic waves has become a mainstream approach, mitigating stress on the structure and enhancing its seismic performance [10-12]. Consequently, the concept of structural vibration control has gradually been integrated into modern structural design, improving the safety and adaptability of structures in resisting both single and sequential earthquakes [13].

Common structural vibration control techniques include passive control, active control, semi-active control, and hybrid control [14-16]. Among these, BRBs have gained popularity in recent decades due to their effective control of structural deformation [17-18]. BRBs are metal energy-dissipating devices, first proposed by Fujimoto et al. in 1988 [19-21]. In addition, Kim et al. [22] performed seismic response analysis of a steel frame structure with BRBs using nonlinear time-history analysis, revealing that the maximum structural displacement tends to decrease as the BRB stiffness increases. Guerrero et al. [23] conducted shaking table tests on two precast RC frames, one strengthened with BRBs and one without, and revealed that BRBs are effective in enhancing structural shear capacity as well as in delaying and reducing stiffness degradation in the precast RC models. Xu et al. [24] applied BRBs to an L-shaped 4-story RC frame and conducted seismic response spectrum calculations as well as dynamic time-history analyses. Their results demonstrated that BRBs significantly enhance the torsional behavior of the RC frame and notably reduce the required amount of reinforcement. Consequently, extensive research has shown that BRBs exhibit exceptional seismic resistance performance.

However, limited reported have considered the failure of BRBs in the seismic response analysis of buckling-restrained braced frame (BRBF). Under sequential earthquakes, BRBF may experiences large residual deformation when BRBs suffer significant plastic deformation [25-26], and BRBs may fracture due to insufficient ductility or accumulated fatigue damage [27]. Kong et al. [28] studied the impact of ultimate deformation capacity of BRBs on the seismic performance of BRBFs. The results indicated that the failure behavior of BRBs can affect the collapse mode of BRBFs, and the seismic response of BRBFs is significantly smaller without considering brace failure. Shu et al. [27] evaluated the influence of earthquake duration on the seismic performance of structures with BRBs, and concluded that earthquake duration has a substantial impact on collapse risk assessment. Therefore, if the initial earthquake is excessively intense, the BRB may incur damage, thereby diminishing its capacity to withstand subsequent seismic events. Additionally, the difficulty in repairing or replacing BRBs during a seismic event can severely compromise structural safety. As a result, identifying an effective damping solution for sequential earthquakes has become a critical challenge.

So far, MRDs have been acknowledged for their low power consumption, fast response, significant damping capacity, and continuous adjustability, establishing them as a valuable tool in structural seismic resistance [29-31]. MRDs feature a large stroke and a simple mechanical design, making them less susceptible to damage. Cha et al. [32] utilized a 200 kN MRD and a performance-based plastic design (PBPD) approach to evaluate the seismic fragility of a controlled 9-story building. The results showed that both the damping device and the PBPD method are highly effective in reducing seismic damage caused by random earthquake ground motions. Dyke et al. [33] conducted the shaking table tests on a 3-story model structure equipped with MRDs. The results indicated that MRDs effectively reduce both the seismic peak response and the root-mean-square (RMS) response of the structure. Li et al. [34] conducted experimental research to evaluate the feasibility of using MRDs for nonlinear seismic control of a three-story steel–concrete hybrid structure. The results confirmed the effectiveness of MR dampers in mitigating structural damage. Behboodi et al. [35] implemented an adaptive control algorithm in combination with MRDs to mitigate low-cycle fatigue damage in building structures subjected to seismic loading. The results indicated that this approach significantly extended the structural fatigue life and improved overall

seismic performance. As described, although BRBs demonstrate excellent seismic resistance, they are susceptible to fracture under sequential earthquakes. In contrast, MRDs offer an extended energy dissipation stroke and high flexibility, enabling real-time modulation of damping behavior to effectively counter seismic excitations.

This study attempts to evaluate the structural damping performance of MRDs under sequential earthquakes, comparing their performance with that of BRBs. The objective is to provide valuable insights for the selection and analysis of dampers in engineering applications. The arrangement of this paper is organized as follows, firstly, a brief research background on the BRBs and MRDs is presented. Section 2 details the establishment of 3- and 9-story simplified models and the selection of earthquake records. The determination of parameters for BRBs and MRDs is discussed in Section 3. Section 4 compares the responses under frequent seismic events. Section 5 compares the responses under rare seismic events, while Section 6 compares the responses under the second rare seismic event. Finally, the main conclusions are summarized.

2. Model establishment

2.1 Establishment of simulation models

To evaluate the control performance of MRDs and BRBs, two reinforced concrete buildings (e.g., 3 and 9-storey structures) are designed following the Chinese seismic codes [36-37]. The buildings are located in a seismic zone with an intensity of 8 (0.30g), site class II, and seismic group II. A 5% damping ratio is assumed for the first two modes. The 3D, plan, and elevation views, along with the structural member dimensions of the frames, are presented in Figure 1. The middle spans of the designed structures are used as the analysis models for comparison.

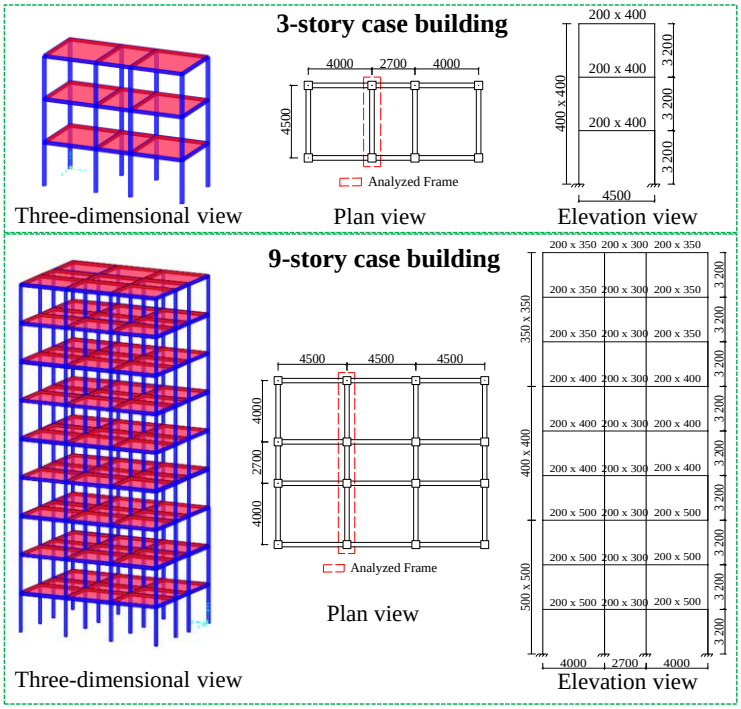

Figure 1. Views of the case study buildings.

The hysteretic behavior of each floor is modeled using the Takeda stiffness degradation model [38], as shown in Figure 2. Post-cracking and post-yielding stiffness degradation coefficients are set to 0.4 and 0.1, respectively. Structural parameters are summarized in Table 1.

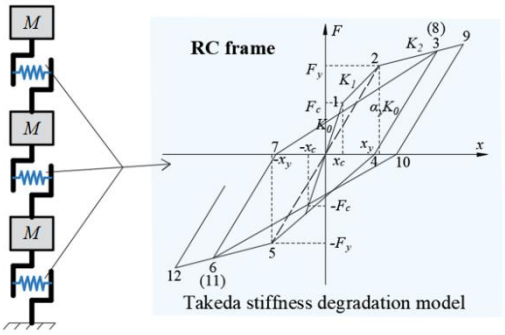

Figure 2: Hysteresis model for each story

Table 1: Parameters for each floor of both structures.

Frame	Floor	M (kg)	K0 (kN m-1)	K1 (kN m-1)	K2 (kN m-1)	xc (mm)	xy (mm)
3-story	1~3	42500	55000	22000	5500	5	16
9-story	1~3	85000	115000	46000	11500	4.5	12
	4~6	75000	103000	41200	10300	4	10.5
	7~9	70000	94000	37600	9400	3.6	9.5

Notes: M = Mass; K_0 = Initial stiffness; K_1 = Cracking stiffness; K_2 = Yield stiffness; x_c = Cracking displacement; x_y = Yield displacement.

The tangent stiffness reduction coefficient α_y at the yield point is calculated as follows:

$$\alpha_y = \frac{F_y}{x_y K_0} \tag{1}$$

MRDs and BRBs are individually installed in the analyzed RC frame to enhance its seismic performance. The elevation views of the RC frames, MRDFs, and BRBFs are shown in Figure 3.

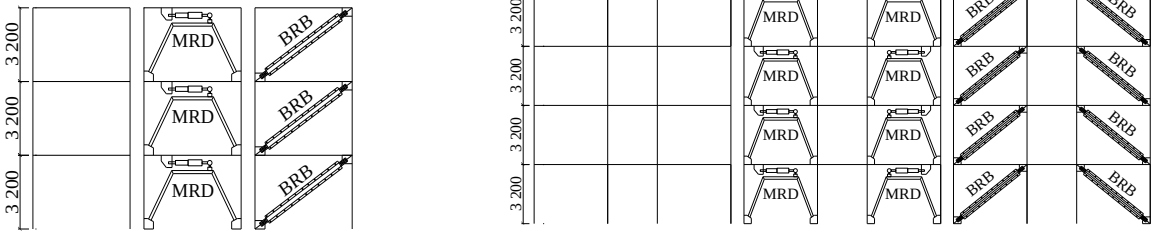

(a) 3-story analyzed frames (b) 9-story analyzed frames

Figure 3. 3- and 9-story RC frames, MRDFs, and BRBFs

2.2 Selection of earthquake records

In accordance with the China Building code [37], two recorded strong ground motion records and one artificial seismic record are selected for each case study frame. The selected natural earthquake records include the Friuli, Taft, Manjil, and Kobe waves, which are used to excite the 3-story and 9-story analytical frames, respectively. The artificial ground motions are generated using the power

spectral density function of the Clough–Penzien model. The peak ground acceleration (PGA) is set to 110 cm/s² for frequent seismic events and 510 cm/s² for rare seismic events. Figure 4 shows the comparison between the standard design spectrum and response spectra of six ground records for 3- and 9-story frames, respectively. The fundamental periods of each case study frame are also indicated and marked on the corresponding spectra. The fundamental periods of 3- and 9-story frames are 0.3925s and 0.9833s, respectively. It can be observed that the differences between the acceleration values corresponding to the fundamental period of each case-study frame in the three response spectra and those of the standard design spectrum remain within 20%. This indicates that the selected ground motion records meet the requirements specified by the design criterion.

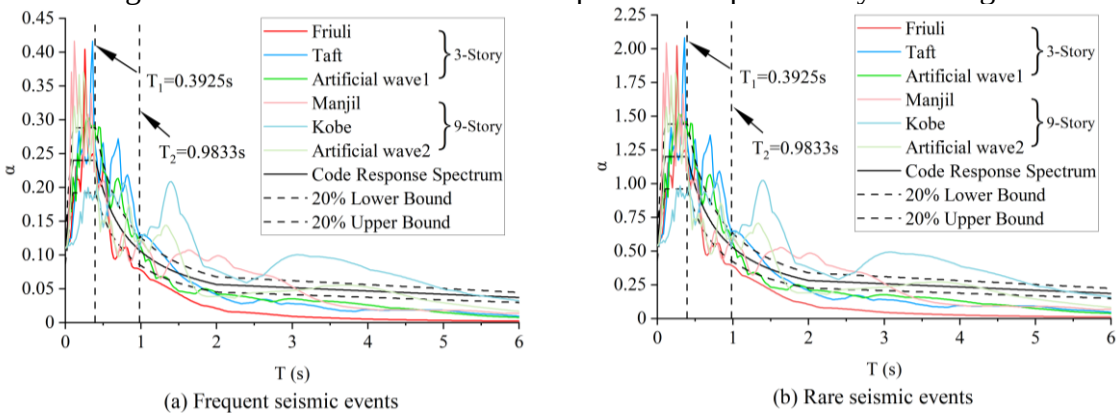

(a) Frequent seismic events (b) Rare seismic events

Figure 4. Response spectra of the six selected earthquake records.

In subsequent analyses, to compare the dynamic response variations of BRBFs and MRDFs under two consecutive rare seismic events and to evaluate their damping effectiveness, an artificial earthquake sequence is constructed using the repetition method [39-40]. Adopting the same ground motion record twice in succession to simulate the sequence of seismic excitations. To accurately evaluate residual displacements, a 10-second unloading phase is appended after each of the two rare seismic excitations. Nonlinear dynamic analyses are subsequently conducted for both consecutive earthquake scenarios.

3. Determination of parameters for BRB and MRD

3.1 Parameters of BRB

A bilinear model is employed to simulate the mechanical behavior of the BRB, with key parameters including initial stiffness K, yield force $F_{BRB,y}$, and post-yield stiffness ratioγ. The parameters are iteratively optimized based on the BRBs' yielding behavior under both frequent and rare seismic events. The design objectives are: (1) under frequent seismic events, the totalstructure remains in the elastic range; and (2) under rare seismic events, the BRBs yield prior to other structural components, entering the plastic stage to dissipate seismic energy in advance [41]. To achieve a 40% reduction in top-floor displacement of the BRBF under frequent seismic events, the BRB parameters are further optimized, as summarized in Table 2.

Table 2: Parameters of the BRBs.

Frame	Floor	K (kN ṁ-1)	FBRB,y (kN)	γ
3-story	1~3	37000	111	0.05
9-story	1~3	72000	216	0.05
	4~6	63000	186	
	7~9	55000	165	

To validate the BRBF modeling approach in MATLAB platform, a three-story frame is analyzed and compared with a corresponding SAP2000 model. The El Centro ground motion record is selected as the input excitation. The nonlinear dynamic analysis of BRBF structures is compared using different simulation methods. The top floor displacement histories are shown in Figure 5, and comparisons of peak displacements and BRB forces at each floor are summarized in Table 3.

As depicted in Figure 5, the time history curves for both models are nearly identical. Additionally, Table 3 shows that the maximum errors in the comparison of peak displacement values and maximum BRB control forces at each floor are 1.36% and 2.41%, respectively. These results demonstrate that both numerical simulations yield highly consistent outcomes. Therefore, the predictive capability of the proposed BRBF modeling approach is validated.

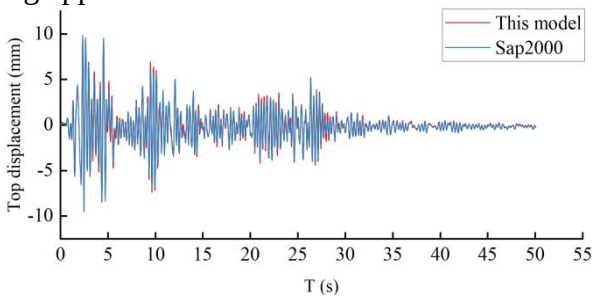

Figure 5. Time histories of the top floor displacements.

Table 3: Comparisons of the maximum displacement values and maximum control forces at each floor.

Floor	Maximum displacement value			Maximum control force		
	This model (mm)	SAP2000 (mm)	Relative error (%)	This model (kN)	SAP2000 (kN)	Relative error (%)
1	5.22	5.15	-1.36	115.20	115.03	-0.15
2	8.14	8.06	-0.99	111.65	111.81	0.14
3	9.81	9.84	0.30	77.75	75.92	-2.41

3.2 Failure criteria of BRB

Although BRBs overcome the instability issues of traditional steel braces under compression, their core elements are susceptible to fatigue damage due to repeated large plastic deformations during energy dissipation. This may lead to fracture failure under rare seismic events.

Cumulative Plastic Deformation (CPD) is defined as the ratio of the total accumulated plastic deformation of a brace during the loading process to its yield displacement. It serves as a critical parameter for evaluating the energy dissipation capacity and is widely recognized as a key indicator of the low-cycle fatigue performance of BRBs [42]. CPD can be expressed as:

$$CPD = \sum_i \frac{|\Delta_{\mathrm{pi}}|}{\Delta_{\mathrm{y}}} \tag{2}$$

Where Δ_{pi} is the i-th plastic deformation segment of the BRB, and Δ_{y} is the yield displacement.

In this study, the maximum CPD of the BRB is set to 200, in accordance with the provisions of AISC 341-16 [42], which specifies this value as the design limit for BRB.

On the other hand, the ductility ratio is defined as the ratio of the ultimate displacement to the yield displacement after yielding. It is another key performance indicator for BRBs under dynamic loads such as earthquakes, commonly used to evaluate their deformability and capacity to sustain plastic deformation. The ductility ratio can be expressed as:

$$\mu = \frac{\Delta_u}{\Delta_y} \tag{3}$$

where μ is the ductility ratio of the BRB, Δ_u is the ultimate displacement, and Δ_y is the yield displacement of BRB.

Previous studies have suggested that the maximum ductility ratio of a BRB should exceed 8 to fully utilize its energy dissipation capacity [28]. In this study, the maximum ductility ratio is set to 12 for the 3-story frame and 9 for the 9-story frame to satisfy this performance criterion.

3.3 Semi-active control of MRD

To simulate the damping characteristics of MRDs, which are capable of rapidly and continuously adjusting their damping properties in response to the structural state, this study employs a Linear Quadratic Regulator (LQR) control algorithm to compute the optimal control force matrix required for the MRDFs. Since the damping force of the MRD is limited and can only provide control forces in the direction opposite to the motion of each story, a semi-active control strategy, as illustrated in Figure 6, is adopted to adjust the optimal control force U to closely approximate the actual output of the MRD [29]. In Figure 6, U_i is the optimal control force of the i-th MRD, $\dot{u}_i$ is the relative velocity at both ends of the i-th MRD, F_i is the damping force of the i-th MRD, F_{min} is the minimum damping forces, F_{max} is the maximum damping forces.

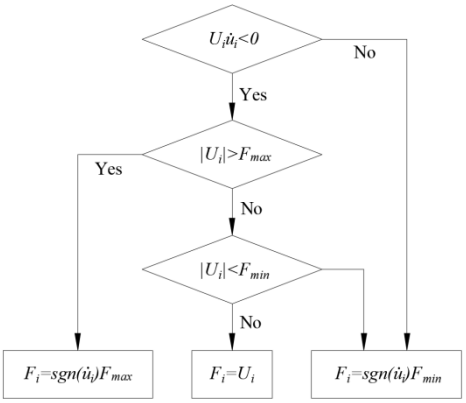

Figure 6. Semi-active control strategy.

To verify the validity of the MRDF modeling procedure developed in MATLAB in this study, and considering that MRDs cannot be simulated directly in SAP2000, the 3-story structural parameters and the weight matrix coefficients for the LQR control algorithm proposed by Ou [15] are adopted and analyzed for comparison. Table 4 presents a comparison of the maximum inter-story drift angles and the MRD control forces for each story. The maximum errors are limited to 1.39% and 2.31%, respectively. This indicates that the MRDF modeling method shows high accuracy in calculating the dynamic behavior of structures.

Table 4: Comparisons of the maximum inter-story drifts and maximum control forces for each floor.

Floor	Maximum inter-story drift			Maximum control force		
	This model (mm)	Ou (mm)	Relative error (%)	This model (kN)	Ou (kN)	Relative error (%)
1	18.25	18.00	-1.39	591.02	587.00	-0.68
2	15.27	15.10	-1.13	468.87	465.00	-0.83
3	8.72	8.70	-0.23	291.58	285.00	-2.31

In this study, the minimum damping force of each MRD is set to 0 kN, while the maximum damping force is defined as the yield force of the BRBs at each story, in order to ensure a fair and

consistent basis for comparison between the two systems. Through a series of trial calculations, the weight matrix coefficients for the LQR control algorithm are determined to be α=100, β=3.1×10^{-5} for the 3-story frame, and α=100, β=1.7×10^{-5} for the 9-story frame, achieving a 40% reduction in top-floor displacement under frequent earthquakes.

4. Comparison of responses under frequent seismic events

4.1 Displacement responses under frequent seismic events

Under the influence of frequent seismic events (a_{pg}=110cm/s^2), the elastic inter-story drift limit θ_e of the reinforced concrete frame structure is 1/550 [37]. The maximum inter-story drifts for both frames are shown in Figs. 7-8. MRDs and BRBs exhibit comparable effectiveness in reducing inter-story drift in both structures.

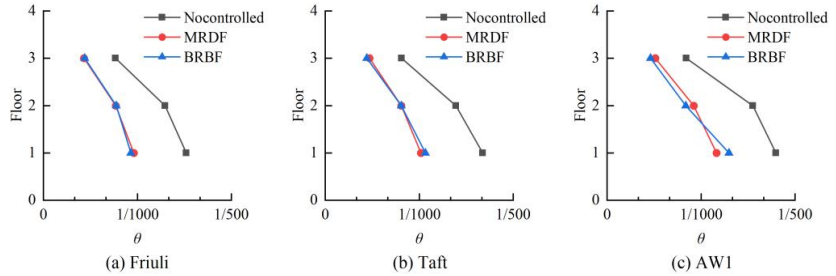

Figure 7. Inter-story drift envelope diagrams for the 3-story frames under frequent seismic events.

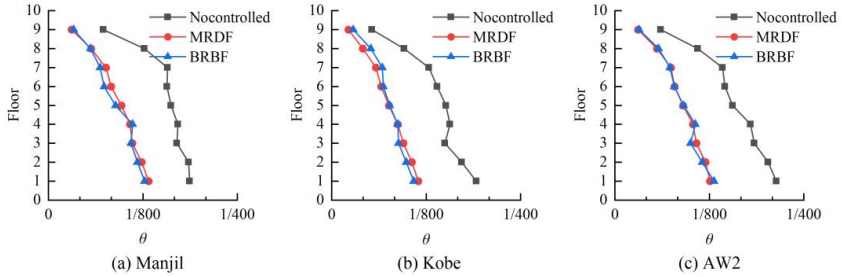

Figure 8. Inter-story drift envelope diagrams for the 9-story frames under frequent seismic events.

Table 5 provides a comparison of the maximum displacement responses of both controlled and uncontrolled frames subjected to frequent seismic events. This comparison includes the maximum drift (θ_{max}) and its corresponding floor, the maximum displacement (Δ_{max}) at the top floor, and the displacement reduction rate. Under frequent seismic events, the maximum drifts of the controlled frames remain within the allowable limit (θ_e), with the maximum drifts occurring at the first floor. The average displacement reduction ratios of the controlled frames under frequent seismic events are approximately 40%, which aligns with the design objectives.

Table 5: The maximum displacement responses of the uncontrolled frames, BRBFs and MRDFs.

Frame	Seismic wave	Uncontrolled frame			BRBF					MRDF				
		θmax	Rel. floor	Δmax (mm)	θmax	Rel. floor	Δmax (mm)	η_Δ (%)	$\bar{\eta}_\Delta$ (%)	θmax	Rel. floor	Δmax (mm)	η_Δ (%)	$\bar{\eta}_\Delta$ (%)
3-story	Friuli	1/658	1F	11.27	1/1075	1F	6.87	39.04	39.55	1/1042	1F	6.85	39.22	39.84
	Taft	1/595	1F	12.33	1/935	1F	7.42	39.82		1/980	1F	7.27	41.04	
	AW1	1/556	1F	13.60	1/769	1F	8.19	39.78		1/862	1F	8.26	39.26	
9-story	Manjil	1/535	1F	41.13	1/785	1F	23.35	43.22	41.63	1/754	1F	25.05	39.09	41.83
	Kobe	1/522	1F	35.55	1/921	1F	19.68	44.65		1/874	1F	20.10	43.45	
	AW2	1/468	1F	38.91	1/763	1F	24.51	37.02		1/795	1F	22.14	43.11	

Notes: η_Δ is the displacement reduction ratio of the controlled structure, $\bar{\eta}_\Delta$ is the average displacement reduction ratio under the influence of seismic waves.

4.2 Acceleration responses under frequent seismic events

Under seismic excitation with a peak acceleration of 110 cm/s ², the floor acceleration responses and top-floor acceleration time histories are shown in Figs. 9-10. The results indicate that both BRBs and MRDs contribute to the reduction of floor acceleration. However, MRDs are more effective in mitigating floor acceleration compared to BRBs. The top-floor acceleration time histories reveal that BRBs amplify the structural acceleration response at certain instances, which could negatively affect structural comfort, whereas MRDs consistently reduce acceleration throughout the entire duration. This can be attributed to the fact that BRBs rarely yield and remain predominantly in the elastic stage, thus failing to dissipate energy. Instead, they increase the structural stiffness, thereby altering its dynamic characteristics. As a result, the structure's sensitivity to seismic spectrum characteristics is altered, leading to occasional amplification of the acceleration response at certain instances.

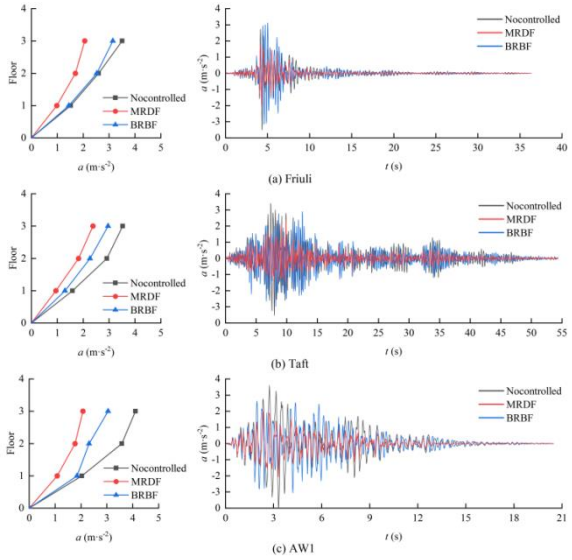

Figure 9: Floor acceleration envelopes and top-floor acceleration time histories of the 3-story frames.

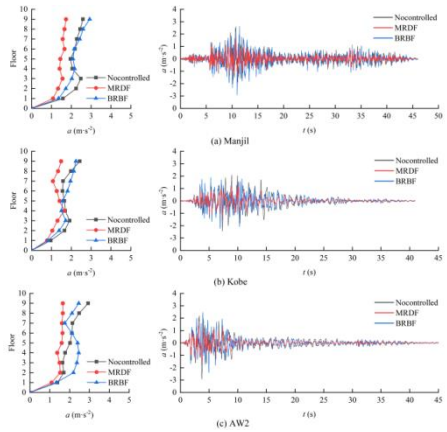

Figure 10: Floor acceleration envelopes and top-floor acceleration time histories of the 9-story frames.

Table 6 presents a comparison of the maximum acceleration responses of the structure under frequent seismic events, including the peak acceleration and its corresponding floor, as well as the acceleration reduction rate. As shown in the table, under frequent seismic events, the maximum

acceleration typically occurs at the top floor. By averaging the analysis results for each seismic wave, the acceleration reduction rate at the top floor of the frame under frequent seismic events is determined. The 3-story BRBF exhibits a reduction rate of 17.32%, whereas the 3-story MRDF shows a reduction rate of 41.11%. Similarly, the 9-story BRBF demonstrates a reduction rate of 3.62%, while the 9-story MRDF achieves a reduction rate of 36.18%. In these comparisons, the MRD proves to be more effective in reducing the structure's acceleration compared to the BRB, enhancing the human comfort of buildings under seismic excitations.

Table 6: Maximum acceleration responses of the uncontrolled frames, BRBFs and MRDFs under rare seismic events.

Frame	Seismic wave	Uncontrolled frame		BRBF				MRDF			
		amax (m s-2)	Rel. floor	amax (m s-2)	Rel. floor	η_a (%)	$\bar{\eta}_a$ (%)	amax (m s-2)	Rel. floor	η_a (%)	$\bar{\eta}_a$ (%)
3-story	Friuli	3.51	3F	3.15	3F	10.26	17.32	2.06	3F	41.31	41.11
	Taft	3.52	3F	2.96	3F	15.91		2.38	3F	32.39	
	AW1	4.11	3F	3.05	3F	25.79		2.07	3F	49.64	
9-story	Manjil	2.59	9F	2.93	9F	-13.04	3.62	1.73	9F	32.98	36.18
	Kobe	2.43	9F	2.24	9F	7.79		1.65	4F	32.10	
	AW2	2.93	9F	2.46	9F	16.12		1.66	9F	43.46	

Notes: a_{max} is the maximum acceleration response, η_a is the acceleration reduction rate for the damping structure, $\bar{\eta}_a$ is the average acceleration reduction rate under the influence of three seismic waves.

5. Comparison of responses under rare seismic events

5.1 Displacement responses under rare seismic events

Under rare seismic events, the elastoplastic inter-story drift angle limit for the RC frame structure is 1/50. The maximum inter-story drift for each floor under seismic excitation with a peak acceleration of 510 cm/s ². In the analysis, a 10-second free-load period is added after each seismic wave time history to obtain a more thorough residual displacements [43]. The 3-story MRDF achieves more effective inter-story drift reduction at the first floor compared to the BRBF. And in the 9-story frame, MRDs offer superior drift control at the 1st and 4th floors, whereas BRBs tend to amplify drifts at these floors. This is mainly due to shear force concentration at the 1st floor and a stiffness irregularity at the 4th floor, which increase the likelihood of BRBs reaching their deformation and CPD limits, resulting in fracture in these critical regions.

The maximum displacement responses of the frames under rare seismic events. The maximum drift (θ_{max}) occurs at the 1st and 4th floors. Kobe wave excitation caused BRB fractures in the 9-story frame, leading to sudden stiffness degradation and first-floor drift exceeding the limit (θ_p =1/50) [37]. This indicates that BRB fractures can result in structural failure, risking severe casualties and major economic losses. The average top-floor drift reduction rates under rare seismic events are 24.99% for the BRBF and 31.00% for the MRDF in 3-story frames, and 24.29% for the BRBF and 31.00% for the MRDF in 9-story frames. It can be observed that, the MRDFs exhibit a slightly better displacement reduction effect compared to the BRBFs. However, when compared to the displacement reduction rates under frequent seismic events, the effect under rare seismic events is reduced, which warrants significant attention in engineering design.

The residual deformation reduction rate of the 3-story BRBF is unstable, especially under the influence of the Friuli and Taft waves. In contrast, the MRDF consistently reduces the top-floor residual deformation and provides better control. The primary cause of this phenomenon is that BRBs, while effectively dissipating energy under strong seismic excitation, also undergo plastic deformation. This inelastic behavior may not fully recover after the event, resulting in increased residual deformation at the top floor. In contrast, the MRDs solely dissipate energy, applying no residual

forces after vibrations cease, thus preventing permanent deformation. In the 9-story frame, both BRBs and MRDs effectively reduce top-floor residual deformation, with MRDs showing better performance.

5.2 Acceleration responses under rare seismic events

The acceleration responses of each floor. Under rare seismic events, both MRDFs and BRBFs experience floor acceleration amplification, with no significant control effect. Compared to the acceleration response under frequent seismic events, the overall acceleration damping effects are reduced.

For the 3-story structures, the average peak acceleration reduction rates are 2.79% for the BRBF and 4.66% for the MRDF. In contrast, for the 9-story frames, negative reduction rates are observed, with -6.19% for the BRBF and -4.46% for the MRDF, indicating an amplification effect on structural response.

5.3. Energy dissipation under rare seismic events

To further compare the state and energy dissipation of BRBs and MRDs in the various layers of the frames, the force-displacement hysteretic curves of BRBs and MRDs under rare seismic events are plotted. Among them, highlights the hysteresis curves of the damping devices in the floors where stiffness variation occurs.

The yield level of the BRB increases as the number of layers decreases, and the BRBs in the top layer have a very small hysteresis curve area, almost no plastic deformation, and remain mostly in the elastic phase, resulting in insufficient energy dissipation. As shown in the figures, after fracture of the BRBs due to fatigue failure or exceeding displacement limit, their damping force remains zero.

Unlike BRB, the displacement and damping force do not reach their maximum values simultaneously. It can be observed that the displacements are largest on the first floor, and the MRDs in the lower floors can reach their maximum damping force during the seismic event. Based on the hysteresis curves, the energy dissipation of each damping device can be obtained Under rare seismic events and considering BRB failure, the seismic energy dissipation in each layer of the MRDs is greater than that of the BRBs.

The average energy consumptions and maximum damping forces of each layer of BRBs and MRDs under different seismic events are calculated. The average maximum damping forces for each layer of BRBs are greater than those of MRDs. However, the seismic energy dissipations of BRBs are lower than that of MRDs. This indicates that MRDs demonstrate superior seismic energy dissipation efficiency, while BRBs primarily function by providing high damping forces to restrict structural displacements.

6. Comparison of responses under the second rare seismic events

6.1 Displacement responses under the second rare seismic events

Following the effects of the initial rare seismic event, a subsequent seismic excitation with a peak ground acceleration of 510 cm/s² is applied. Furthermore, a 10-second zero-load interval is appended to the end of each seismic time history. The maximum inter-story drifts and floor displacements for each story of the 3-story and 9-story structures. In BRBs-fractured stories, MRDs exhibit a clear advantage by offering enhanced safety and more effective control of structural response.

The maximum inter-story drifts and top-floor displacements of BRBFs are consistently greater than those of MRDFs across all seismic events. The peak inter-story drifts typically occur at the 1st

or 4th floor. On average, the top-floor displacement is reduced by 15.29% in the 3-story BRBF and by 32.87% in the 3-story MRDF. For the 9-story frames, the reduction rates are 19.56% and 28.30%, respectively. Compared to the first rare seismic event, both systems exhibit increased inter-story drifts and top-floor displacements during the second event; however, the BRBFs show a more significant amplification, indicating potential safety concerns.

By calculating the top-floor residual displacement reduction rates and response amplification ratios, MRDFs demonstrate more stable control in reducing top-floor residual deformation compared to BRBFs. Compared to the top-floor residual deformations after the first seismic event, the residual deformations of the 3-story frames increase following the second seismic event, whereas the top-floor residual deformations of the 9-story frames do not show a consistent increase.

6.2 Acceleration responses under the second rare seismic events

The acceleration responses of each floor, as well as the top floor acceleration time histories, were analyzed for both the 3-story and 9-story frames under the second rare seismic event. The results indicate that an acceleration amplification phenomenon occurred, which is consistent with the behavior observed during the first rare seismic event.

The maximum acceleration responses of each frame under the second rare seismic event were compared. The maximum acceleration of the 3-story structure occurs at the top floor, whereas that of the 9-story structure does not. The average maximum acceleration reduction rates for the 3-story BRBFs and MRDFs are 4.52% and 9.72%, respectively, while those for the 9-story BRBFs and MRDFs are 7.31% and 4.49%, respectively. It can be observed that during the second rare seismic events, MRDs and BRBs have a negligible impact on acceleration response.

6.3 Energy consumption under the second rare seismic events

To compare the performance and energy dissipation of BRBs and MRDs at each story, force–displacement hysteretic curves are analyzed. The responses under the Taft and Kobe ground motions are selected respectively and are presented. The certain BRBs failed during the first seismic event and thus did not contribute during the second event, whereas BRBs on other floors remained functional. In contrast, the lower-level MRDs are more likely to reach their maximum damping force, with larger hysteretic loops, indicating more effective energy dissipation.

Compares the energy dissipation E_i of BRBs and MRDs at each story, along with the corresponding ratio R_i relative to the first earthquake. As shown in the table, under the second rare earthquake excitations and considering BRB failure, the energy dissipation in each story of the MRDs exceeds that of the BRBs, indicating superior performance of the MRDs. Analyzing the energy dissipation data reveals that both BRBs and MRDs show a significant reduction in energy dissipation on the upper floors compared to the first earthquake.

For the second seismic events, the average maximum damping force of BRBs and MRDs at each story are calculated under various earthquake inputs. Excluding stories with BRBs fracture, the average maximum damping force of MRDs is lower. Considering both rare seismic events, MRDs show more stable and sustained energy dissipation, while BRBs mainly rely on higher damping forces to reduce structural vibrations.

7. Conclusion

This study evaluates the seismic mitigation performance of MRDs in 3- and 9-story frames subjected to sequential earthquake excitations, and compares their effectiveness with that of BRBFs. Numerical models of MRDFs and BRBFs are developed in MATLAB, accounting for possible BRB

failure modes. The stability and effectiveness of MRDs under repeated seismic loading are verified through nonlinear dynamic time-history analyses. Seismic performance is assessed based on maximum inter-story drift, top-floor displacement, residual deformation, peak acceleration, and energy dissipation capacity. The key findings are summarized as follows:

1) Under the condition of maintaining the same top-floor displacement reduction rate for frequent seismic events, MRDs have been found to outperform in mitigating structural acceleration responses, with reductions of 30% to 50%, thereby improving occupant comfort. In contrast, BRBs exhibit limited effectiveness in mitigating peak acceleration, with average reduction rates of only 17.32% and 3.62% for the 3-story and 9-story frames, respectively. More critically, the analytical results indicate that, under certain dynamic loading conditions, BRBs may inadvertently amplify acceleration responses.

2) Comparative analysis under sequential rare seismic events indicates that MRDs provide superior control of inter-story drift compared to BRBs, achieving reductions ranging from 20% to 40%. Notably, on certain floors where BRBs fracture, the inter-story drift partially exceeds the allowable limit, posing a potential risk of structural failure. In contrast, MRDs effectively mitigate the occurrence of this phenomenon, thereby enhancing the safety of life and property. Furthermore, MRDs significantly reduce residual deformation at the top story of the frames, while BRBs may even exacerbate it.

3) During two consecutive rare seismic events, both BRBs and MRDs exhibit enhanced energy absorption at lower story levels. While BRBs generate higher damping forces, MRDs demonstrate superior energy dissipation efficiency and more stable hysteretic behavior throughout the excitation.

4) Compared to the structural responses analyzed during the initial seismic events, the maximum displacement responses of all frame structures generally exhibited amplified trends under the second identical earthquake excitations. Notably, the peak acceleration of the 3-story BRBF exhibited a general decrease. Moreover, the cumulative energy dissipation capacities of both upper-level BRBs and MRDs in the 3-story and 9-story frames demonstrated reduced performance during the subsequent seismic events.

References

[1] Zhao B, Taucer F, Rossetto T. Field investigation on the performance of building structures during the 12 May 2008 Wenchuan earthquake in China. Engineering Structures, 2009, 31(8): 1707-1723.

[2] Liu L, Zhao D S, Zhu Y, et al. Spatiotemporal characteristics of earthquake hazard losses in mainland China during 1993-2017. Journal of Natural Disasters, 2021, 30(03) :14-23.

[3] Hatzigeorgiou G D, Liolios A A. Nonlinear behaviour of RC frames under repeated strong ground motions. Soil Dynamics and Earthquake Engineering, 2010, 30(10): 1010-1025.

[4] Raghunandan M, Liel A B, Luco N. Aftershock collapse vulnerability assessment of reinforced concrete frame structures. Earthquake Engineering & Structural Dynamics. 2015.44(3): 419-439.

[5] Hatzivassiliou M, Hatzigeorgiou G D. Seismic sequence effects on three-dimensiona reinforced concrete buildings. Soil Dynamics and Earthquake Engineering, 2015, 72(5): 77-88.

[6] Shu S, Dai K, Li T, et al. Impact of ground motion duration on seismic performance of buckling restrained braced frames. Soil Dynamics and Earthquake Engineering, 2023, 174: 108197.

[7] Amiri G G, Rajabi E. Effects of consecutive earthquakes on increased damage and response of reinforced concrete structures. Computers and Concrete, An International Journal, 2018, 21(1): 55-66.

[8] Wen W, Zhang M, Zhai C, et al. Resilience loss factor for evaluation and design considering the effects of aftershocks. Soil Dynamics and Earthquake Engineering, 2019, 116: 43-49

[9] Hou L Q, Dong S E, Gao Y Y, et al. Comparative analysis of seismic isolation, energy dissipation, and conventional seismicresistance. Earthquake Resistant Engineering and Retrofitting, 2011, 33(02): 50-56.

[10] Almajhali K Y M, He M, Alhaddad W. Enhancing seismic performance of structures: A comprehensive review of hybrid passive energy dissipation devices. Structures, 2024, 69: 107223.

[11] Harvey Jr P S, Kelly K C. A review of rolling-type seismic isolation: Historical development and future directions. Engineering Structures, 2016, 125: 521-531.

[12] ZHU X L, LIN M Q, GAO R, et al. Research Progress in the Application of Seismic Isolation Technology in China. North China Earthqauke Sciences, 2020, 38(4): 86-91.
[13] Yao J T. Concept of structural control. Journal of the Structural Division, 1972, 98: 1567-1574.
[14] Yan W M, Zhou F L, Tan P. Research advances in vibration control of civil engineering structures. World Earthquake Engineering, 1997, (02): 8-20.
[15] Ou J P. Structural vibration control – active, semi-active, and intelligent control. Beijing: Science Press, 2003.
[16] Li A Q. Vibration control of engineering structures. Beijing: China Machine Press, 2007.
[17] Zhao J, Zhang J, Song J, et al. Sliding gusset connections for improved seismic performance of BRB-RC frame: Damage-control design and subassemblage tests. Engineering Structures, 2023, 282: 115828.
[18] Cao X Y, Feng D C, Wu G. Pushover-based probabilistic seismic capacity assessment of RCFs retrofitted with PBSPC BRBF sub-structures. Engineering Structures, 2021, 234: 111919.
[19] Fujimoto M, Wada A, Saeki E, Watanabe A, Hitomi Y. A study on the unbonded brace encased in buckling-restraining concrete and steel tubes. Journal of Structural and Construction Engineering (Trans AIJ) 1988;34B:249–58 [in Japanese)].
[20] Fujimoto M, Wada A, Saeki E, Watanabe A, Hitomi Y. A study on brace enclosed in buckling-restrained mortar and steel Tubes (Part 1). Japan, October: Annual Research Meeting Architectural Institute of Japan, Kanto Area; 1988 (in Japanese).
[21] Fujimoto M, Wada A, Saeki E, Watanabe A, Hitomi Y. A study on brace enclosed in buckling-restrained mortar and steel tubes (Part 2). Japan, October: Annual Research Meeting Architectural Institute of Japan, Kanto Area; 1988 (in Japanese).
[22] Kim J, Choi H. Behavior and design of structures with buckling-restrained braces. Engineering Structures, 2004, 26(6): 693-706.
[23] Guerrero H, Ji T, Escobar J A, et al. Effects of buckling-restrained braces on reinforced concrete precast models subjected to shaking table excitation. Engineering Structures, 2018, 163: 294-310.
[24] Xu B, Chen A J, Chen Z P, et al. Shock absorption effect analysis of buckling restrained brace applied to reinforced concrete frame. Earthquake Resistant Engineering and Retrofitting, 2016, 38(03): 118-123.
[25] Tremblay R, Lacerte M, Christopoulos C. Seismic response of multistory buildings with self-centering energy dissipative steel braces. Journal of Structural Engineering, 2008, 134(1): 108-120.
[26] Erochko J, Christopoulos C, Tremblay R, et al. Residual drift response of SMRFs and BRB frames in steel buildings designed according to ASCE 7-05. Journal of Structural Engineering, 2011, 137(5): 589-599.